Gas Target Characterization at OPAL

Contact: linus.feder@physics.ox.ac.uk

L. Feder, J. Chappell, J. Cowley, E. Archer, S. Kalos, D. McMahon, W.Wang, R. Walczak, & S.M. Hooker

John Adams Institute for Accelerator Science and Department of Physics, University of Oxford, Denys Wilkinson Building, Keble Road, Oxford OX1 3RH, United Kingdom

Abstract

Plasma fluorescence measurements were performed for two different multi-centimetre laser wakefield targets. These measurements demonstrate the usefulness of this technique for target characterization. The gas cell target was shown to be uniform, while the gas jet target was shown to have a density dip of ∼20%.

Introduction

Development of novel gas targets is an important element of laser wakefield accelerator (LWFA) experiments. For guided LWFAs, gas targets that provide uniform gas densities over tens of centimeters are needed, with densities in the range 10^{17} – 10^{18} cm^{-3}, near the detection limit of the standard diagnostic, transverse interferometers. At the Oxford Plasma Accelerator Laboratory (OPAL) we have performed plasma fluorescence measurements [1] to characterize the longitudinal gas density profile within the long gas targets used in our two most recent experiments with the Gemini laser in Target Area 3 (TA3). These targets were: (i) a 110-mm adjustable gas cell [2, 3] and (ii) a 40 mm-long slit jet [in preparation].

The most common method of characterizing gas targets is interferometry, but most interferometric methods rely on cylindrical symmetry to extract a three-dimensional (3D) gas density profile from the 2D phase shift recorded by a probe beam. Transverse interferometric methods also typically require high spatial resolution and high sensitivity to detect the lower gas densities required for high-energy acceleration. This limits the field-of-view, meaning that many measurements are needed to determine the longitudinal profile of a long target. The long length of the target also makes the phase shift too high for a longitudinal probing geometry.

In the plasma fluorescence technique, a short pulse laser (central wavelength 800 nm, pulse duration 45 fs) was focused by an axicon lens to form a plasma column along the axis of the target. Fluorescent light from the plasma was imaged by a fixed focal length lens onto a 16-bit CMOS sensor (Andor Zyla 5.5, 10 ms exposure time). First, for each target, a separate calibration dataset was recorded to measure the longitudinal plasma fluorescence as a function of a known, uniform gas pressure. This was achieved by back-filling the entire target chamber with the relevant gas over a range of pressures (see Fig. 1). At each pressure, the plasma fluorescence for ten consecutive events was measured. These indicated shot-to-shot fluorescence fluctuations of approximately 15%, likely dominated by the laser energy jitter (∼10%). The measured signal was integrated transversely over the region of the plasma fluorescence, and averaged over the ten events, to extract the fluorescence intensity as a function of gas pressure at each longitudinal position, z, as shown in Fig. 1 (b). Then, for each z, the measured fluorescence as a function of pressure was fit to a seventh-order polynomial to estimate the relation between gas pressure and fluorescence, F (z, P). An example of this is shown in Fig. 1 (e).

To estimate the longitudinal gas pressure profile generated during experiments, the chamber was evacuated and the longitudinal plasma fluorescence was recorded when the target was operated in a pulsed mode, with gas valve opening times and laser arrival times matching those used in experiments. Again, ten events were recorded per configuration. The measured longitudinal plasma fluorescence was converted to a longitudinal gas pressure profile via inversion of the calibration functions found previously. The total uncertainty on the reconstructed gas pressure at each longitudinal position includes contributions from the uncertainty on the polynomial fit to the calibration curves combined with the shot-to-shot fluctuations of the plasma fluorescence measured in pulsed operation mode.

This setup was used to characterize two different targets: a 110 mm-long adjustable gas cell and a 40 mm-long slit jet, shown in Fig. 1 (a). The longitudinal variation of the intensity profile of the axicon foci are shown in Fig. 1 (c) and 1 (d). The differences in the measurement parameters are shown in the table below.

Parameter	**Gas cell**	**Slit jet**
Laser pulse energy [mJ]	120 ± 10	240 ± 20
Axicon base angle [deg]	2.5	4.5
Gas species	H_2	He + 2% Ar
Calibration range [mbar]	0 - 35	0 - 100

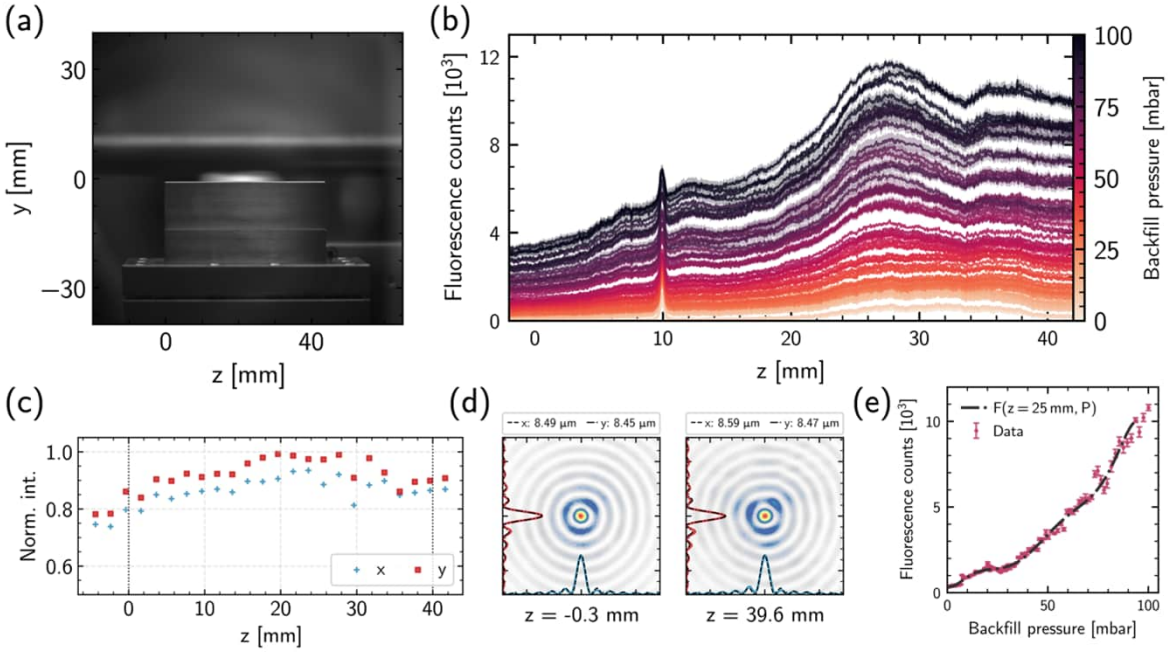

Figure 1: (a) Image of the 40 mm-long slit jet in place at OPAL; (b) example calibration curves demonstrating the measured average longitudinal fluorescence as a function of the backfill pressure; (c) measurements of the normalised peak intensity of the axicon focus at the position of the slit-jet; (d) measured axicon focal spots at either end of the slit-jet, with fits to the transverse intensity profiles; (e) example backfill calibration curve for z = 25 mm.

The axicon angle, longitudinal axicon intensity variations, laser energy and gas species do not have a significant effect on the accuracy of the measurement. The only effect of these differences is in the degree of ionization and amount of fluorescence produced, but in both cases these differences will be present in both the calibration data and signal data. The backfill fluorescence calibration data taken for the 40 mm-long slit jet is shown in Fig. 1 (b). As long as the fluorescence intensity at each position has a monotonic relationship with backfill pressure, the pressure function F (z, P) can be found and the measurement performed. Fig. 1 (e) shows an example plot of F (z, P) for the z = 40 mm position in the gas cell experiments.

Gas cell measurements

Figure 2 shows the results of these measurements for the 110 mm-long gas cell. The raw fluorescence signal, averaged over ten events, is shown in Fig. 2 (c), from which the gas pressure can be estimated via inversion of the calibration functions. The resulting normalized pressure profile is shown by the data points in Fig. 2 (a), and is compared to a calculation of the expected pressure profile predicted by fluid simulations. The measurements are consistent with the simulations and indicate a uniform longitudinal profile, with fluctuations of 4.1% RMS observed. The relative uncertainty on the measurement increased with z since this region of the focus was generated by light in the transverse wings of the incident laser beam, which was more susceptible to laser energy and pointing jitters. In addition, the fluorescence signal in this region was significantly weaker, reducing the signal-to-noise ratio and increasing the fit uncertainty in the calibration data. The relative fluctuation in the measured fluorescence profile in pulsed operation mode was typically on the order of 15%, similar to backfill operation, and indicates that no further significant fluctuations were introduced in pulsed operation mode. The dominant contribution to the shot-to-shot fluctuations observed during these measurements was therefore consistent for both datasets and was likely a result of the laser energy jitter.

Gas jet measurements

Figure 3 shows the equivalent results for the slit jet. The longitudinal pressure profile was measured for backing pressures in the range 10 – 70 bar, at two different heights above the gas slot (Δy): 3 mm (Fig. 3 (a)) and 5 mm (Fig. 3 (b)). As expected, the pressure recorded above the slot increased with increasing backing pressure, with a peak pressure of approximately 90 mbar measured 3 mm above the slot when using a backing pressure of 70 bar, corresponding to an atomic density of helium in excess of 2 x 10^{18} cm^{-3}. The average pres-

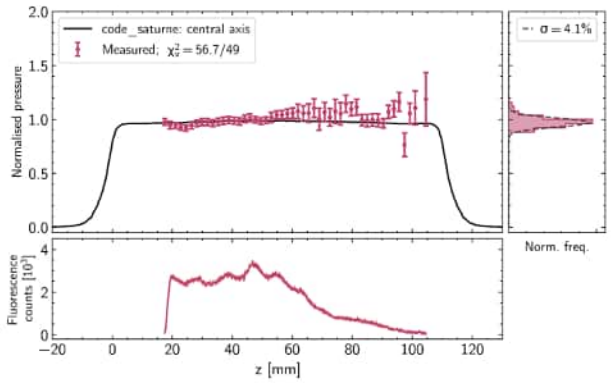

Figure 2: (a) Measurement of the pressure of the gas cell vs longitudinal position, along with the predicted profile from fluid simulations; (b) histogram of the measurements; (c) raw fluorescence signal from the cell.

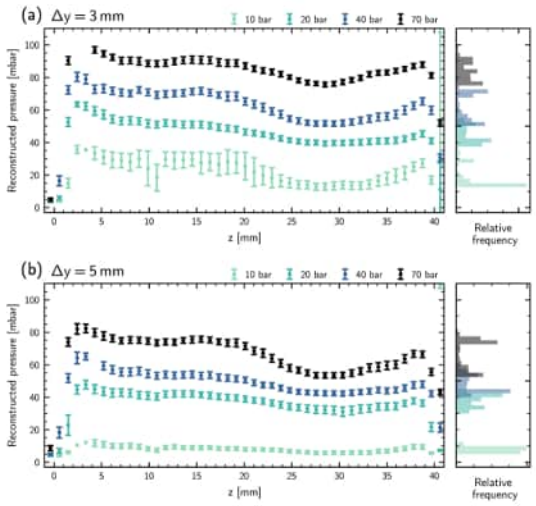

Figure 3: (a) Pressure 3 mm above the 4 cm slit jet for different backing pressures, with histograms on the right; (b) the same data for 5 mm above the jet.

sure decreased with increasing height above the jet, but atomic densities in excess of 1 x 10^{18} cm^{-3} were still accessible 5 mm above the jet, over the entire length of the jet. In all cases, and particularly at higher backing pressures, a dip in gas pressure was observed at $z \sim 30$ mm. This gradient in gas density inferred from the fluorescence was confirmed by interferometric measurements conducted at RAL [4], and was attributed to a partial obstruction of the nozzle throat which was removed before experimentation in TA3. As shown in Fig. 3, data were taken at both 3 mm and 5 mm above the jet, with different calibration curves for each height. In principle, more heights could be taken and the fluorescence function F could be extended to also include a height y.

Conclusion

The plasma fluorescence technique is a simple and powerful method for measuring the longitudinal density profile of long gas targets. It can be easily adapted to higher resolutions or larger field of view by changing the imaging of the fluorescence camera. The technique is usable with many different laser and pumping systems, relatively simple to setup and gives accurate and quick results.

References

[1] B. Miao *et al.* Multi-GeV Electron Bunches from an All-Optical Laser Wakefield Accelerator. *Phys. Rev. X*, **12**, 031038 (2022).

[2] A. Picksley *et al.* All-Optical GeV Electron Bunch Generation in a Laser-Plasma Accelerator via Truncated-Channel Injection. *Phys. Rev. Lett.*, **131**, 245001 (2023).

[3] A. J. Ross *et al.* Resonant excitation of plasma waves in a plasma channel. *arXiv:2310.05097*, (2023).

[4] O. J. Finlay *et al.* Gas Target Design and Characterization for EPAC EA1. *in this report.*